Available online at www.sciencedirect.com
ScienceDirect
Thin Solid Films 516 (2008) 2934 – 2938
thin solid films
www.elsevier.com/locate/tsf

Phase transformation and optical characteristics of porous germanium thin film

T.S. Ko [a,*], J. Shieh [b], M.C. Yang [b], T.C. Lu [a], H.C. Kuo [a], S.C. Wang [a]

[a] Department of Photonics & Institute of Electro-Optical Engineering, National Chiao Tung University,1001 Tahsueh Rd., Hsinchu 30050, Taiwan, ROC
[b] National Nano Device Laboratory, 26 Prosperity Road I, Science-based Industrial Park, Hsinchu 30078, Taiwan, ROC

Received 30 May 2006; received in revised form 12 April 2007; accepted 5 June 2007
Available online 14 June 2007

Abstract

In this study, we proposed a method to prepare GeO_2 by treating porous Ge thin film with thermal annealing in O_2 ambient. After annealing, the morphological transformation from porous thin film to an island structure was observed. The crystallization and composition of the porous Ge thin film prepared using different annealing time in O_2 ambient were confirmed by X-ray diffraction, X-ray photoelectron spectroscopy and Raman spectra. Initial Ge composition was gradually oxidized to GeO_2 with increasing annealing time. Comparing the photoluminescence (PL) results between Ge and GeO_2, it was found that the visible photoluminescence originated from the germanium oxide. Photoluminescence measurements obtained at different temperatures exhibited a maximum integrated PL intensity at around 200 K. A possible explanation for this behavior might be the competition between radiative recombination and nonradiative hopping process.
© 2007 Elsevier B.V. All rights reserved.

Keywords: Chemical vapor deposition; Germanium; Phase transitions; Photoluminescence

1. Introduction

Since the observation of visible luminescence, nanostructured silicon and germanium have attracted much attention recently. For example, visible photoluminescence (PL) characteristics of SiGe nanostructure with high area to volume ratio can be achieved at room temperature [1–3]. These nanostructured materials have excellent potential for applications on optical-electronic devices [4]. The earliest room-temperature luminescence for silicon was discovered from porous silicon prepared by electrochemical anodization in a dilute hydrofluoric acid solution [5]. Because bulk silicon is a semiconductor with indirect band gap energy about 1.12 eV (1100 nm), it is generally believed that the PL emission in visible light segment originated from either quantum confined effect or capture of excitons from the interface between surface oxidization film and Si crystal [6]. In contrast to silicon, germanium has lower energy band gap energy about 0.67 eV and larger effective excitonic Bohr radius so that the quantum confined effect related to limit size could be easier achieved [7].

To date many relevant researches on luminescence property of SiGe system have been carried out. For example, Liu et al. have fabricated self-organized Ge quantum dot superlattices by solid source molecular beam epitaxy, and they observed the blue shift emission peak from the decreasing size of quantum dots [8]; Zhu et al. have fabricated Si and Ge nanocrystals in Ge/Si thin film prepared by using a variation of the pulsed laser deposition method, and studied the possibility of light emission from interface between the crystal and thin film [9]; Zacharias et al. have investigated the luminescence in SiO_2 films containing Ge and GeO_2 nanocrystals [10]. In spite of many methods that have been developed to prepare nanostructured Ge materials and the optical properties that have been intensively studied, it is still not clear how the visible luminescence mechanism originated from either defects in oxide or interface between nanocrystal and oxide, even quantum confinement effects.

Recently, we have reported that high quality porous Ge thin film can be prepared by low-pressure inductively coupled plasma chemical vapor deposition (ICPCVD) [11]. In this study, we

* Corresponding author. Tel.: +886 3 5712121x52962; fax: +886 3 5716631.
E-mail address: tsko.eo93g@nctu.edu.tw (T.S. Ko).

0040-6090/$ - see front matter © 2007 Elsevier B.V. All rights reserved.
doi:10.1016/j.tsf.2007.06.023

further focused on porous Ge thin film, which was treated with thermal annealing for different time. The surface morphology was observed by scanning electron microscopy (SEM). The crystallization and composition of porous Ge thin film from different annealing time were confirmed by X-ray diffraction (XRD), X-ray photoelectron spectroscopy (XPS) and Raman spectra. These results demonstrated that porous Ge thin film capped with a germanium oxide layer was gradually oxidized to GeO_2 with increasing annealing time. PL spectra showed that the emission peak positions in visible light region were identical for both nanostructured porous Ge and GeO_2, which revealed that GeO_2 contributed to the visible PL emission. The photoluminescence was also measured at various temperatures to investigate the emission mechanisms.

2. Experimental details

The Si substrates cleaned with water were immersed in a 3-Aminopropyl-trimethoxysilan (APTMS) ethanol solution of 1 mM for 45 min, followed by washing with ethanol and water. The Si substrates then were dipped in the solution of gold nanoparticles which were produced by the chemical reduction of gold chloride tetrahydrate ($HAuCl_4$) with sodium citrate. The gold nanoparticles with 20 nm in diameter and 1.46×10^{11} cm^{-2} in density were linked to the native Si dioxide layer by the self-assembled monolayer of APTMS. After dipping process, the substrates were cleaned by deionized water and then were baked at 100 °C for 5 min. The wafer was afterward loaded into the ICPCVD chamber. Before deposition, the gold-coated silicon substrate was cleaned by 200 cubic centimeter per minute (sccm) oxygen plasma at 350 °C for 10 min and 200 sccm hydrogen plasma at 400 °C for 5 min in the same ICPCVD chamber, and the deposition chamber was evacuated to $<6.65\times10^{-3}$ Pa. We began to grow by using 1 sccm of pure GeH_4 and 200 sccm of H_2 as the reactants. The growth temperature, radio frequency plasma power, 300 kHz bias power and working pressure were 400 °C, 500 W, 300 W, and 1.333 Pa, respectively. The samples were then furnace-annealed at the temperature of 500 °C for 3, 5, and 10 min in O_2 ambient.

The morphological features of all samples were investigated by field-emission scanning electron microscopy (SEM, JEOL 6500F) at a vacuum 5×10^{-4} Pa. The operating voltage of our SEM analysis was 10 keV. The structure was analyzed by typical ω-2θ X-ray diffraction (XRD, Philips X'pert Pro), using monochromatic Cu Kα radiation. The chemical bonding of porous Ge thin film from different annealing time was investigated by X-ray photoelectron spectroscopy (XPS, VG Microlab 310F) with a concentric hemispherical analyzer. The pressure inside the chamber was of the order 10^{-8} Pa; Al K_α radiation (1486.6 eV) was used in a fixed analyzer transmission mode (the pass energy was 20 eV). The beam energy was 15 kV and the beam current was 20 mA, and the analyzed area was 2 mm × 5 mm. The C 1*s* line (284.5 eV) was used as a reference to correct charge shift. There is no sputtering before analysis because the X-ray beam size is much larger than the ion beam size. Auger electron spectrometry (AES, VG Microlab 310F) was also used to obtain the composition depth profile, in which etching was performed by utilizing argon ions (Ar^+) with 3 kV beam energy and 105 mA emission current. The crystallinity of the samples was also measured by Raman spectroscopy. An Ar ion laser with 488 nm incident wavelength and 150 mW output power was used as the excitation source of the laser Raman scattering spectrometer. The scattered light was collected in the backscattering geometry. For PL measurements, samples were excited with a continuous-wave 325 nm He–Cd laser at a power density of 20 mW cm^{-2}. The emission light was dispersed by a spectrometer and collected by a CCD detector. The prepared samples were placed in a vacuum chamber of 1.333 Pa attached to a closed-cycle Helium refrigerator for temperature variation (10–298 K).

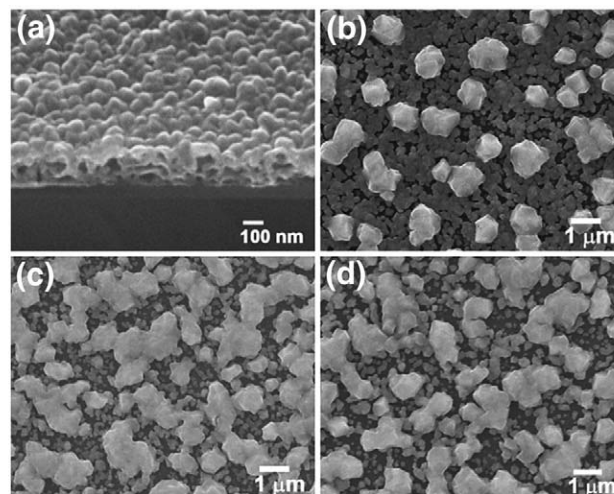

Fig. 1. SEM image of the porous Ge thin film with different annealing time. (a) 0 min, (b) 3 min, (c) 5 min and (d) 10 min.

3. Results and discussion

Fig. 1(a)–(d) show the SEM images of the porous Ge thin film with different annealing time. Fig. 1(a) shows a typical SEM image of the porous Ge thin film, prepared by ICPCVD at 400 °C for 1 h. In this process, Au nanoparticles were used as a catalyst for vapor–liquid–solid growth mechanism, in which GeH_4 preferred to react with Au nanoparticles to form the Au–Ge alloy, and then precipitate Ge from the alloy. Au nanoparticles may be removed by high density plasma during the growth of the porous layer because we did not find them by TEM, EDS and AES analyses after growth [11]. Porous structure was created after following lateral growth and deposition on the protruding islands. The composition of the porous layer was pure Ge and the surface was covered with a germanium oxide layer, as identified by AES; the depth analysis revealed that no Au atoms are detectable through the layer of porous Ge. Fig. 1(b)–(d) illustrate the porous thin film annealed with 3, 5, and 10 min annealing process, respectively. Clearly the initial porous structure disappeared and aggregated lumps of the islands structure. The size of the island structure aggregated was about 1 µm from Fig. 1(b). With increasing annealing time, the size of island structure congregated gradually caused the area of the Si substrate to be larger. The Raman results presented in Fig. 2 reveal that for the sample without annealing treatment only one Raman peak can be clearly

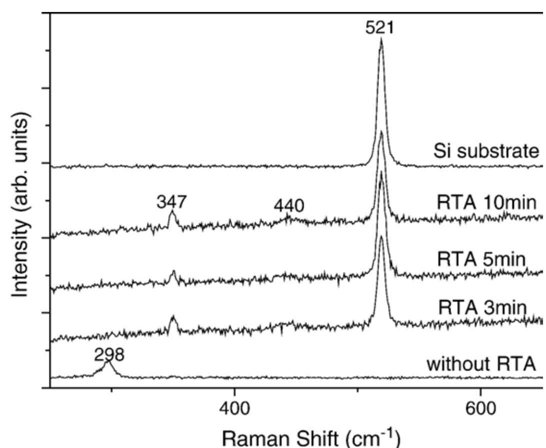

Fig. 2. Raman spectrum analyses of the porous Ge thin film with different annealing time.

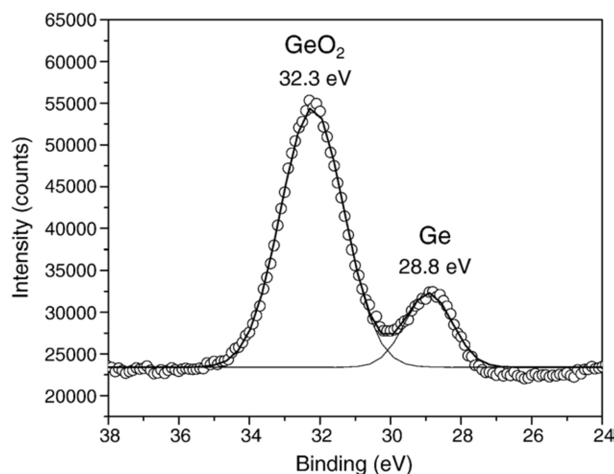

Fig. 4. XPS result of the Ge_{3d} core levels of the porous Ge thin film.

observed at 298 cm^{-1}, which was the feature for the existence of Ge–Ge optical mode [12]. Kolobov pointed out that the feature around 300 cm^{-1} might come from the Si substrate instead of Ge–Ge mode [13]. However, our Raman spectrum of the pure Si (*c*-Si) substrate shown in Fig. 2 only exhibited the peak of 521 cm^{-1}. Recently, Mei et al. [14] grew Ge nanorod on porous anodic alumina template by utilizing saturated vapor adsorption, and demonstrated that the peak of 300 cm^{-1} was attributed to the Ge bonding by comparing the Raman spectra of Ge nanorods and bulk Ge. Therefore, we suggested that the peak of 300 cm^{-1} in our experiment should come from the porous Ge layer. The peak of 521 cm^{-1} from crystalline Si was not detected in the porous Ge sample because the intensity of the Ar^+ laser could not reach the Si substrate and most of the Raman scattering light was absorbed by the porous Ge thin film. Others with annealing treatment show that three peaks included 347 cm^{-1}, 440 cm^{-1} and 521 cm^{-1}. The vanished peak of 298 cm^{-1} indicated Ge–Ge bonds decomposition due to annealing process and demonstrated that the pure Ge composition has changed. The peak of 521 cm^{-1} indicated a crystal bulk Si. It is interesting to note that the peak of 347 cm^{-1} did not come from the substrate scattering, implying that some new Ge-related bonds formed except for the change of the composition of the porous Ge thin film. In the previous studies, Choi et al. have fabricated Ge nanocrystal by annealing Ge ion implanted silicon dioxide [15], and Kartopu *et al.* have studied Raman spectra of SiGe nanocrystals [16]; nevertheless they did not find the peak of 347 cm^{-1}.

Fig. 3 shows the XRD results of the samples with different annealing time. The sample without annealing exhibited the peaks of 27.4°, 45.3° and 53.9°, representing Ge(111), Ge(220) and Ge (311), respectively. After annealing process, the peaks indicating crystal GeO_2 instead of those initial Ge-related peaks [17,18] demonstrated that the Ge constituent transferred into GeO_2 after a 500 °C annealing process. Wu et al. have analyzed the XRD spectra of Ge/PS (porous Si) and demonstrated that the peak of 347 cm^{-1} in Raman spectra may come from the scattering of tetragonal Ge nanocrystals [19]. Although our Raman spectra of the sample after annealing also exhibited the peak of 347 cm^{-1}, the XRD results showed no Ge constituent within those samples. We suggested that the peak of 347 cm^{-1} should relate to Ge–O composition or structure instead of tetragonal Ge nanocrystals. In Fig. 4, an XPS result of the Ge 3*d* of the sample shows that germanium was partially oxidized and the porous Ge was capped

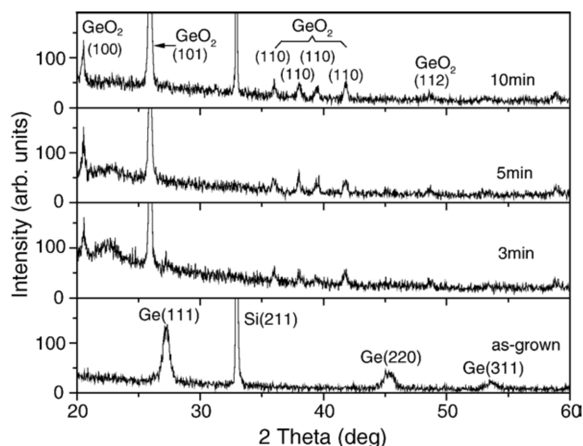

Fig. 3. XRD analyses of the porous Ge thin film with different annealing time.

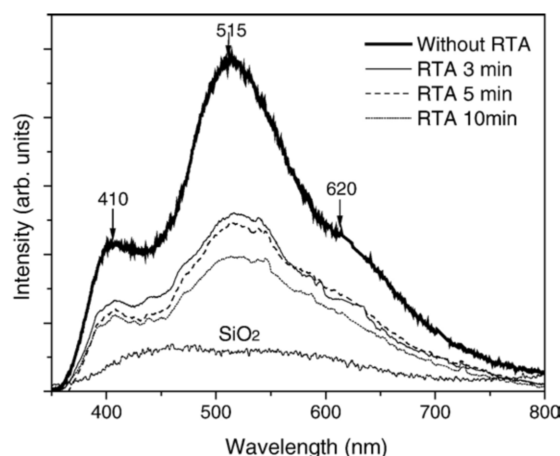

Fig. 5. Room temperature photoluminescence spectra of the porous Ge thin film with different annealing time.

with an oxide layer. The difference in binding energy between Ge–Ge and Ge–O (3.5 eV) was consistent with the reference value for GeO_2. There is no diffraction peak of GeO_2 in XRD analyses indicating that the germanium oxide is characterized with an amorphous structure. The observed germanium oxide was developed after the growth of the porous germanium thin film.

We measured the PL spectra of the samples with different annealing time at room temperature in order to investigate the effect of annealing on optical characterizations and emission mechanisms. The PL spectra of all samples after annealing presented in Fig. 5 reveal three peaks including one center at 515 nm and two shoulders at 410 nm and 620 nm. Moreover, the intensity also decreased. Gao et al. ruled out the emission probability of quantum confinement in visible region on Ge nanocrystals, and indicated that 410 nm (~3.1 eV) can be attributed to the triplet to singlet transition in GeO_2 defects containing two non-bonding electrons [10,20]. There are two origins for the 515 nm and 620 peaks. One is the defect in oxide, such as SiO_2 or GeO_2. Another is the interfacial defect between Si/SiO_2 and Ge/SiO_2. We grew SiO_2 on Si substrate and further measured PL spectrum to clarify above issues, as shown in Fig. 5. This low intensity spectrum curve of SiO_2, which was dissimilar to other spectrum curves, could demonstrate that the vacancies in SiO_2 and Si/SiO_2 interface should not cause the emission peaks as the other sample did. Because most Ge disappeared after annealing, the interface contribution could also be ruled out. Consequently, we believed that these emissions came from the vacancies in GeO_2. In addition, compared to the porous Ge sample, the decreased intensity in annealing samples demonstrated that the defects in native amorphous germanium oxide were more than those in crystal GeO_2.

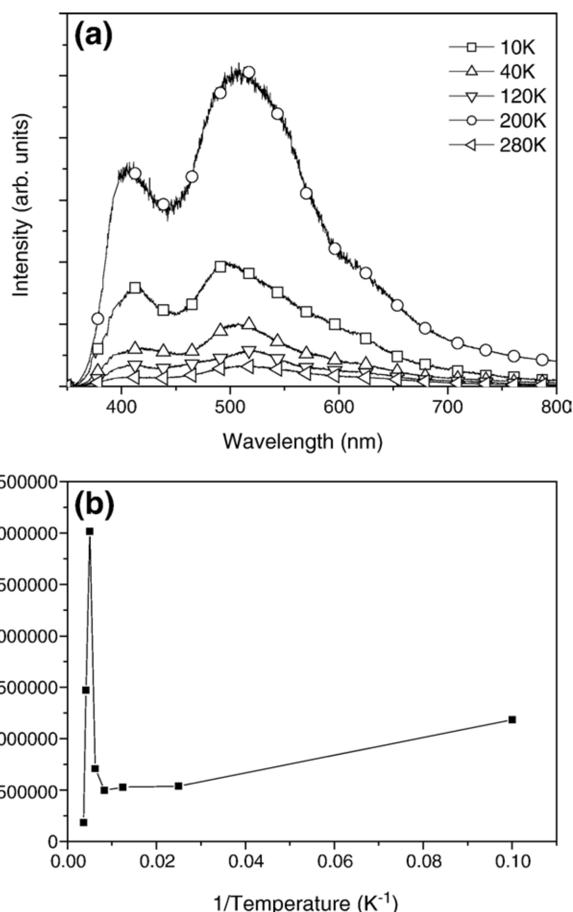

Fig. 6. (a) PL spectra measured at various temperatures for the porous thin film. (b) Integrated PL intensity of the 515 nm peak versus the different inverse measurement temperatures.

In Fig. 6(a), the PL spectra were obtained at various temperatures for the porous thin film, in which the three PL peaks show a slight blue-shift at lower temperature. Fig. 6(b) shows the integrated PL intensity as a function of 1/T for the visible emission in porous Ge which reaches maximum at the temperature of 200 K. This result indicates that the decay dynamic for the electron-hole pairs generated in the germanium oxide exhibits a competition between a thermal active Arrhenius type radiative recombination and a Berthelot type nonradiative hopping escape recombination rate. Carrier transport in the porous Ge predominantly follows a surface mechanism. The similar behavior for temperature dependence of the luminescence in porous silicon has been reported in an earlier literature [21] but has never been discussed for porous germanium. Based on our experiment results, we suggested that the radiative recombination is low at low temperature below 200 K, on the other hand, the hopping escape rate is high at higher temperature than 200 K. Further analysis and research must be confirmed by combining with decay time obtained by using time resolved PL.

4. Conclusion

In summary, we have investigated the phase transformation and optical characteristics of the porous Ge thin film and the GeO_2 particles along with the annealing process. The SEM images showed that the porous morphology of a Ge thin film transferred into an island structure after 500 °C annealing. The XRD and Raman spectra results demonstrated that most Ge molecules transferred into GeO_2 after the porous Ge thin film was treated with the annealing process. The PL results showed that the visible emission of the porous Ge thin film was originated from the germanium oxide. The temperature dependence PL spectra revealed that the electron-hole pair in germanium oxide might be due to the competition between radiative recombination and nonradiative hopping processes.

Acknowledgement

We thank Prof. W. F. Shieh and T. C. Huang for the assistance on the Raman instrument and useful discussions. The study was supported by the MOE ATU program and, in part, by the National Science Council of the Republic of China under contract nos. NSC 95-2120-M-009-008, NSC 95-2752-E-009-007-PAE, and NSC 95-2221-E-009-282.

References

[1] V. Yam, V.L. Thanh, Y. Zheng, P. Boucaud, D. Bouchier, Phys. Rev., B 63 (2001) 033313.
[2] J.P. Wilcoxon, G.A. Samara, Appl. Phys. Lett. 74 (1999) 3164.

[3] D.C. Paine, C. Caragianis, T. Shigesato, T. Ishikawa, Appl. Phys. Lett. 62 (1993) 2842.
[4] S. Hayashi, K. Yamamoto, J. Lumin. 70 (1996) 352.
[5] L.T. Canham, Appl. Phys. Lett. 57 (1990) 1046.
[6] R.T. Collins, P.M. Fauchet, M.A. Tischler, Phys. Today 50 (1997) 24.
[7] Y. Maeda, N. Tsukamoto, Y. Yazawa, Y. Kanemitsu, Y. Masumoto, Appl. Phys. Lett. 59 (1991) 3168.
[8] J.L. Liu, G. Jin, Y.S. Tang, Y.H. Luo, L.L. Wang, D.P. Yu, Appl. Phys. Lett. 76 (2000) 586.
[9] Y. Zhu, C.L. Yuan, S.L. Quek, S.S. Chan, P.P. Ong, J. Appl. Phys. 90 (2001) 5318.
[10] M. Zacharias, P.M. Fauchet, Appl. Phys. Lett. 71 (1997) 380.
[11] J. Shieh, H.L. Chen, T.S. Ko, H.C. Cheng, T.C. Chu, Adv. Mater. 16 (2004) 1121.
[12] M.I. Alonso, K. Winer, Phys. Rev., B 39 (1989) 10056.
[13] A.V. Kolobov, J. Appl. Phys. 87 (2000) 2926.
[14] Y.F. Mei, Z.M. Li, R.M. Chu, Z.K. Tang, G.G. Siu, R.K.Y. Fu, P.K. Chu, W.W. Wu, K.W. Cheah, Appl. Phys. Lett. 86 (2005) 021111.
[15] S.H. Choi, S.C. Han, S. Hwang, Thin Solid Films 413 (2002) 177.
[16] G. Kartopu, S.C. Bayliss, Y. Ekinci, E.H.C. Parker, T. Naylor, Phys. Status Solidi, A Appl. Res. 197 (2003) 263.
[17] T. Lange, W. Njoroge, H. Weis, M. Beckers, M. Wuttig, Thin Solid Films 365 (2000) 82.
[18] P. Viswanathamurthi, N. Bhattarai, H.Y. Kim, M.S. Khil, D.R. Lee, E.K. Suh, J. Chem. Phys. 121 (2004) 441.
[19] X.L. Wu, Y. Gu, G.G. Siu, E. Fu, N. Tang, T. Gao, X.M. Bao, J. Appl. Phys. 86 (1999) 707.
[20] T. Gao, S. Tong, X.Q. Zheng, X.L. Wu, L.M. Wang, X.M. Bao, Appl. Phys. Lett. 72 (1998) 3312.
[21] L.T. Canham, Appl. Phys. Lett. 57 (1990) 1046.